ON MARINE LIABILITY PORTFOLIO MODELING

BY

WILLIAM GUEVARA-ALARCÓN (iD), HANSJÖRG ALBRECHER (iD) AND PARVEZ
CHOWDHURY

ABSTRACT

Marine is the oldest type of insurance coverage. Nevertheless, unlike cargo
and hull covers, marine liability is a rather young line of business with claims
that can have very heavy and long tails. For reinsurers, the accumulation of
losses from an event insured by various Protection and Indemnity clubs is an
additional source for very large claims in the portfolio. In this paper, we first
describe some recent developments of the marine liability market and then sta-
tistically analyze a data set of large losses for this line of business in a detailed
manner both in terms of frequency and severity, including censoring tech-
niques and tests for stationarity over time. We further formalize and examine
an optimization problem that occurs for reinsurers participating in XL on XL
coverages in this line of business and give illustrations of its solution.

KEYWORDS

Marine insurance, extreme value theory, Pareto distribution, optimal reinsur-
ance.

1. INTRODUCTION

Marine is the oldest line of business in insurance. It goes back to the ancient
civilizations of Babylonians, Greeks, and Romans. These societies had systems
of maritime loans to shipowners on their ships and cargo. The borrowed money
would then be paid back with interest in case the journey went well or the loans
would be forgiven in case of a loss of the ship. Rhodian shipowners included in
their law the principle of "general average." This principle allowed to propor-
tionally share losses among several shipowners, when the losses were needed
to preserve the rest of the merchandise in the case of an emergency. The first
documented reinsurance contract dating from 1370 relates to the cargo of a
ship sailing from Genoa to the harbor of Sluis, for which the most dangerous

part of the trip from Cadiz to Sluis was reinsured. For a detailed description of the history of marine insurance, see Holland (2009), Swiss Re (2003). Marine insurance has naturally evolved substantially since then and it is nowadays commonly divided into four classes of business: cargo, hull, offshore energy, and liability. Previous works as Swiss Re (2003), Farr *et al.* (2014), Seltmann (2019) describe the principal features and methods used in these classes, the marine insurance market place in general, the important role of the London market in it, as well as the exposure management that is required to control the potential accumulation risk of single events. Cargo traditional coverage comprises the goods and merchandise that is carried by the vessels. Hull protects against damages happening to the structure and machinery of the vessels. In contrast, offshore energy and liability are rather young markets in marine insurance, appearing at the end of the nineteenth century. Offshore energy involves the protection of platforms, semi-submersibles, and drill ships that carry out exploration and production of oil in the sea. Finally, marine liability provides financial support to shipowners and charterers from the risks of legal liabilities. The difficulties that data availability can pose to price contracts in this market are noted in Farr *et al.* (2014), particularly for contracts covering the higher layers where only very limited claim experience is available.

One distinguishes two types of coverage provided in the marine liability insurance market. On the one hand, Protection and Indemnity (P&I) clubs are mutuals that group together shipowners, ship operators, and charterers to pool their risks and provide coverage against their legal liabilities to third parties for their members. Because of the high limits of liability, particularly involving pollution, P&I clubs also pool their risks via the International Group of P&I clubs (IGP&I), the trade association of the P&I clubs. The IGP&I coordinates the clubs pooling agreement and administers the General Excess of Loss (IG GXL) Reinsurance Contract on behalf of the clubs. The IG GXL is a common reinsurance program transferred to the commercial market to cover the highest losses to which the club members are exposed. On the other hand, commercial (re)insurance companies additionally offer coverage for third-party liabilities on a fixed-premium basis as well as protection for the higher layers of the risks covered by P&I clubs (for instance, also by participating in the previously mentioned IG GXL Contract). The magnitude of total claims can be enormous (e.g., in the case of Costa Concordia exceeding a billion US$) and the settlement of some claims can take more than a decade.

After describing some recent developments in the marine liability insurance market in Section 2, the focus of the remaining paper is twofold: we first give a statistical analysis of a set of actual large losses from this line of business in Section 3, modeling both the size of the claims and their frequency. Section 4 then describes the general framework of an insurance market in the presence of a big reinsurance program, involving many companies, designed to cover the largest market claims. Section 5 introduces several variants of resulting profit optimization problems for reinsurers in this market, who participate in a large excess of loss (XL) reinsurance contract (as the IG GXL mentioned

above) and in addition reinsure individual cedents that also participate in it. In Section 6, we give illustrations of possible solutions to these problems and Section 7 concludes.

2. Marine Liability Insurance Market

During the last decade, IGP&I club premiums (known as "calls") have represented between 61% and 67% of the total marine liability premium. They amounted to US $3 billion in 2018 while commercial insurer's marine liability premiums accounted for US $1.9 billion in the same year, according to Seltmann (2019). Marine liability coverage offered by commercial insurers on a fixed-premium basis represented around 10% of the total P&I calls in 2011 as noted in Futterknecht *et al.* (2013). These figures highlight the central role that P&I clubs play in the marine liability insurance market. In fact, P&I clubs appeared in the second half of the nineteenth century to cover open-ended liability risks that commercial insurers were reluctant to underwrite. Nowadays, the IGP&I gathers 13 P&I clubs and covers around 90% of the world fleet, cf. Futterknecht *et al.* (2013), IGP&I (2017). The 13 clubs retain losses below an individual club's retention (at US $10 million in 2019), while the claims between US $10 and US $100 million are covered by Hydra, the captive of IGP&I, and the claims above US $100 million are reinsured in the open market (see Section 4 for further details).

Regarding the frequency of marine liability large losses, it is expected to continue to decrease in the future. Shipping is now safer than ever, the number of total shipping losses of vessels over 100 gross tonnage per year have fallen from 207 in 2000 to 46 in 2018 (AGCS, 2019). In addition, ITOPF (2019) illustrates that the number of oil spills of more than 700 tons has also decreased from an average of 24.5 per year in the 70s to 1.9 per year after 2010. In fact, 19 of the 20 largest spills registered since 1970 occurred before 2000 (ITOPF, 2019). This indicates that even with the relentless growth of the world fleet, not only the relative frequency of maritime accidents, but also the absolute number of large oil spills has dropped. Similar to motor and aviation transport, human error is the main reason for marine casualties. Human error is the cause of 75–96% of marine incidents according to AGCS (2019) or 70–80% of incidents according to IGP&I (2017). The arrival of autonomous vessels in the coming decades could hence contribute to a further reduction of marine accidents, much like the expected decrease in the number of automobile claims.

Conversely, the size of marine liability large losses seems to increase, see Lloyds (2013), AGCS (2019). Firstly, vessels have been continuously increasing in size. The latest container ships can carry more than 20,000 twenty-foot equivalent units (TEU), which is more than 6 times the capacity of MV Rena (3351 TEU), which ran aground in New Zealand in 2011 (constituting one of the most expensive historical liability losses). These larger ships lead to new and complex challenges regarding the evacuation and rescue in remote

environments. They are also harder to handle and the removal of their wrecks takes longer due to lack of salvage equipment and technology capable of removing them. Secondly, the cost of wreck removal has risen during this century due to various reasons such as the increase in vessel size and cargo volumes. Technological advances also permit carrying out wreck removals in more challenging and more extreme environments than before, but the costs associated with these can be immense compared to past removals. Central factors to the cost of wreck removal are: the location of the incident, cargo recovery from container ships, bunker fuel removal operations, and the influence of government or other authorities, see Lloyds (2013). The last one, strengthened by increasing environmental concern and media coverage, appears to be the dominant factor. For instance, in the case of the Costa Concordia incident, the Italian government required the wreck to be removed in one piece and to carry out the removal work entirely in Italy which substantially increased the cost of the operation. Finally, the most expensive marine liability losses are typically also associated with another factor, namely the cleaning and environmental costs when oil was spilled on the ocean. The quantity of oil spilled is relevant but as White and Molloy (2003) indicate, this is not the only determining factor to the cost of oil spills. Important in this context are also the type of oil, the location and the characteristics of the affected area.

3. MODELING MARINE LIABILITY LARGE LOSSES

We now analyze a data set collecting the information on the most expensive marine liability claims from eight insurance companies, that occurred between 2007 and 2017, obtained from a global reinsurance company. This set of claims includes mainly oil spills, wreck removals, collisions of two or more vessels, groundings, and fires on board. The amounts were reported in 2018 and have been indexed to reflect costs at the end of that year. The consumer price index (CPI) from the United States was used for loss indexation. Although this is a simplified approach, US CPI was chosen as a proxy for global claims inflation considering the global nature of the exposures in this line of business. It is in fact challenging to find an index that reflects the different factors influencing this line of business, the heterogeneous mix and global spread of the claims, the effect of local court decisions and jurisdictional practice. We have information on the date of the incidents, paid and incurred amounts. Ultimate amounts for claims that are still open have been computed applying age-to-age development factors following the chain-ladder method until the seventh year of development and fitting a Weibull logarithmic curve to estimate the loss development tail factors above the eighth year. The data set gathers aggregate claim costs across the eight companies for each single event with indexed incurred values above US $2.85 million. Marine liability losses caused by natural catastrophe events such as hurricanes, earthquakes, wildfires, or tsunamis, as well as energy liability losses involving oil rigs, are excluded from the analysis. Natural catastrophe events are not considered because

they are not one of the main drivers of the costliest marine liability claims as it is the case for the cargo and hull coverages. Additionally, these risks are usually evaluated by means of commercial catastrophe models that do not use past claim experience per se. The data set has a total of $n = 85$ combined claims of which 26 are closed. These large claims are shared among several companies. In fact, half of the claims (43) affected at least two companies, and four claims (among them the two most expensive, Costa Concordia and MV Rena) even involve seven of the eight companies. In the following, we analyze the frequency and severity of this data set of claims, using the methodology recently described in Albrecher *et al.* (2017).

3.1. Frequency modeling

It is usual to examine the number of claims per year when modeling the frequency of claims. In such a case, generalized linear models or generalized additive models with a Poisson or negative binomial response are the common choice. Nevertheless, in our case, the data set seems to be too small to provide a useful model along these lines, given the low frequency registered over the 11-year period.

3.1.1. *Homogeneous Poisson process.*

We proceed to use the additional information on the exact date of the incidents, to model the number of claims $N(t)$ up to time t as a stochastic process. We use days as the time unit, having observed 4018 days in the 11-year period. First, we test for a homogeneous Poisson process, with estimated intensity of $\hat{\lambda} = 85/4018 = 0.0212$ claims per day. We test the hypotheses of exponential inter-arrival times and of a uniform distribution of arrival times over the entire period. These hypotheses are not rejected for this data set when the Anderson–Darling (0.75 and 0.51 p-values) and the Kolmogorov–Smirnov (0.83 and 0.7 p-values) tests are applied, which indicates that the homogeneous Poisson process could be seen as a reasonable model for the claim arrival process. Figure 1 shows the exponential QQ-plot of the inter-arrival times as well as the actual claim counts over time together with the simulated 95% confidence interval for the homogeneous Poisson process based on 10,000 realizations. Although the tests do not reject the distributional hypotheses on the inter-arrival and arrival times at this usual significance level, the QQ-plot still exhibits some deviation from the exponential distribution, particularly for larger inter-arrival times. Hence, the hypothesis of a constant intensity during the 11-year period, a key property of the homogeneous Poisson process, still may not be the most reasonable choice.

3.1.2. *Inhomogeneous Poisson process.*

We hence explore the fit of an inhomogeneous Poisson process with intensity function $\lambda(t)$ changing over time. A Gaussian kernel estimator for the intensity
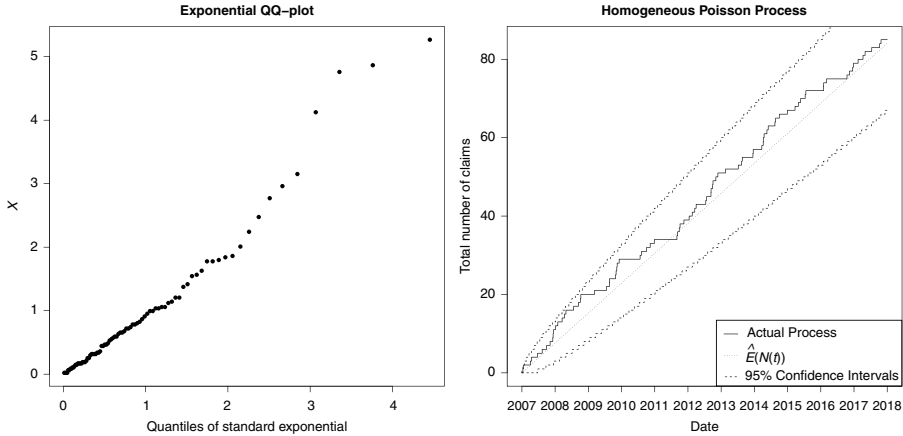
FIGURE 1: QQ-plot of the standardized inter-arrival times (left) and simulated 95% confidence intervals for a homogeneous Poisson process with $\hat{\lambda} = 0.0212$ and observed cumulative count claims (right).

function using the arrival times T_i is used as, for example, proposed by Diggle (1985)

$$\hat{\lambda}(t) = \frac{1}{h} \sum_{i=1}^{n} K\left(\frac{t - T_i}{h}\right). \tag{3.1}$$

Pseudodata built through reflection at the boundaries $t_0 = 0$ and $T = 4018$ of the observed arrival times (see e.g., Cowling and Hall, 1996) are used to correct for underestimation of $\lambda(t)$ near the boundaries. The bandwidth h is chosen applying the extensively used plug-in method in Sheather and Jones (1991), giving $h = 887$ as a result. Alternative plug-in and cross-validation methods to determine the bandwidth give similar results with $h \in [680, 970]$, however, $h = 360$ (an annual standard deviation) and $h = 180$ are also considered.

A second alternative consists of using a log-linear intensity function given by

$$\hat{\lambda}(t) = \exp\left(\theta_0 + \theta_1 t\right), \tag{3.2}$$

whose maximum likelihood estimators (MLEs) are equal to $\hat{\theta}_0 = -3.674$ and $\hat{\theta}_1 = -0.00009$. The negative value of the parameter θ_1 suggests a decrease in the claims frequency over time. However, when testing the null hypothesis $H_0 : \theta_1 = 0$, through the likelihood ratio test with respect to the homogeneous model, we obtain a p-value of 0.32, indicating no evidence to reject the hypothesis that the process has constant intensity.

A third alternative consists of using a piecewise constant function composed by the annual estimated intensities. Figure 2 (top left) shows the occurrence dates of the claims (in the rug) as well as the estimated intensity function $\hat{\lambda}(t)$ using a Gaussian kernel of the form (3.1) with the mentioned
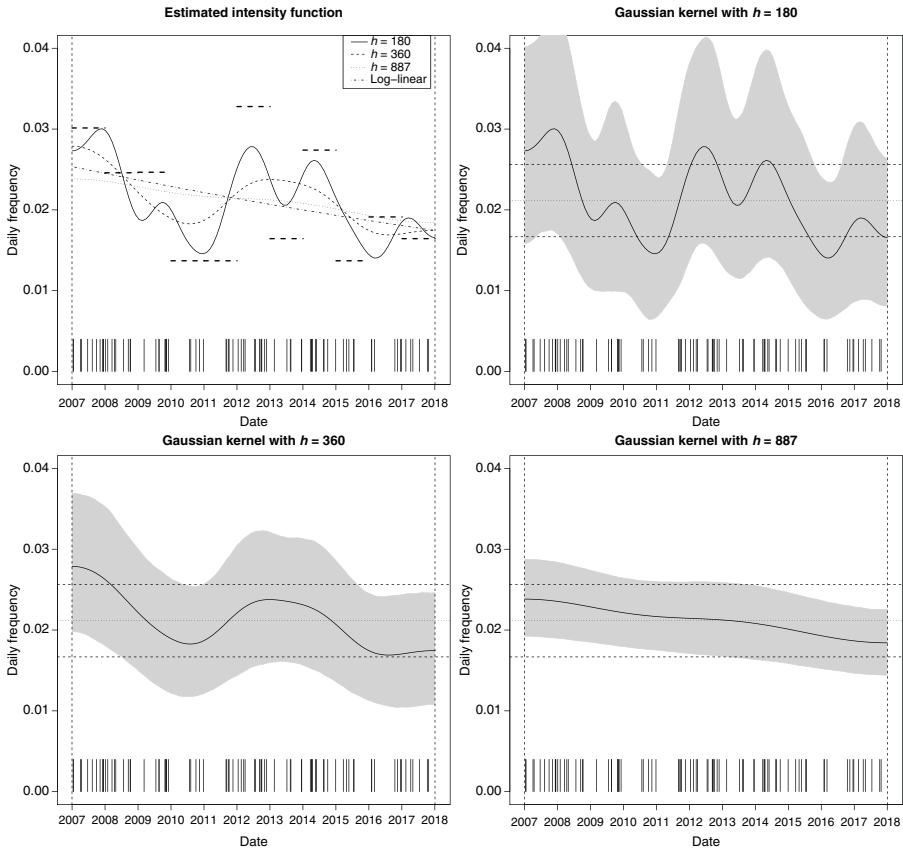
FIGURE 2: Estimated Poisson intensity function $\hat{\lambda}(t)$ using a Gaussian kernel with $h = 180, 360, 887$, log-linear intensity and annually constant values (top left). Remaining plots: 95% confidence intervals of the homogeneous intensity estimate $\hat{\lambda} = 0.0212$ and the inhomogeneous intensity estimate for each bandwidth.

values for the bandwidth ($h = 180, 360, 887$), the log-linear intensity in (3.2), and the piecewise (annually) constant function. The estimated function using the kernel exhibits a decreasing pattern over time, being monotone decreasing for the largest bandwidth $h = 887$ while having additional periodic fluctuations for the shorter bandwidths.

The confidence intervals at 95% level for the inhomogeneous intensity estimators $\hat{\lambda}(t)$ in Figure 2 are computed following the procedure in Merz *et al.* (2016), see also Albrecher *et al.* (2019). For the homogeneous intensity, the 95% confidence interval is derived from the estimates of 10,000 samples of exponential inter-arrival times with mean $1/\hat{\lambda}$. The confidence intervals around the inhomogeneous intensity estimate $\hat{\lambda}(t)$ turn out to always contain the homogeneous estimate $\hat{\lambda} = 0.0212$. On the other hand, the confidence interval of the homogeneous intensity contains the inhomogeneous estimate for $h = 887$, and
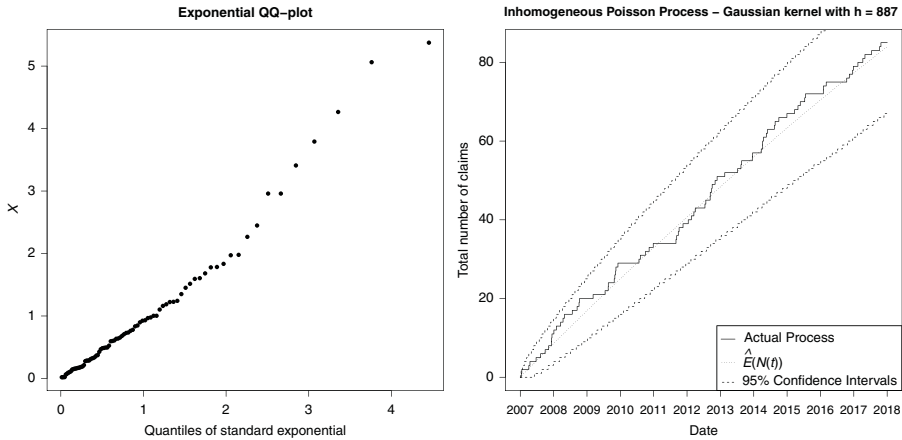
FIGURE 3: QQ-plot of the standardized inter-arrival times after time change (left) and simulated 95% confidence intervals for an inhomogeneous Poisson process with $\lambda(t)$ estimated with Gaussian kernel $h = 887$ and observed cumulative count claims (right).

the estimates for the other bandwidths fall outside of the interval. This suggests that despite a visible decreasing pattern of the intensity, the data set is not rich enough to conclude such a decrease decisively at the usual significance level.

For the sake of completeness, we still test in the following whether for a given inhomogeneous Poisson estimate the inhomogeneous Poisson assumption would be justified. For that purpose, we apply a deterministic time change to the inter-arrival times using the estimated intensity $\hat{\lambda}(t)$ with bandwidth $h = 887$, so that the resulting process should then follow a homogeneous Poisson pattern, and then repeat the above tests. In this case, the hypotheses of exponential inter-arrival times and uniform arrival times under the new timescale are not rejected for both Anderson–Darling (*p*-values 0.82 and 0.93) and Kolmogorov–Smirnov (*p*-values 0.89 and 0.94) tests. Figure 3 shows the exponential QQ-plot of the transformed inter-arrival times and simulated confidence intervals for the inhomogeneous Poisson process using $\hat{\lambda}(t)$ as in (3.1) with $h = 887$, and Figure 4 depicts the corresponding results for the piecewise (annual) constant intensity. One observes that the QQ-plot constitutes an improvement over the one under the homogeneous Poisson assumption in both cases. Autocorrelation functions, partial autocorrelation functions, and Ljung Box tests suggest also independence of the inter-arrival times.

To summarize, we observe a better fit of the inhomogeneous Poisson process to the data set as a claim arrival model, showing a decreasing behavior of the intensity function over time, as expected from general considerations on decreasing likelihood of incidents in this line of business. However, there is always a trade-off with respect to model complexity, and the statistical tests to rule out the homogeneous Poisson process turned out not to be conclusive for the 11 years of data available.
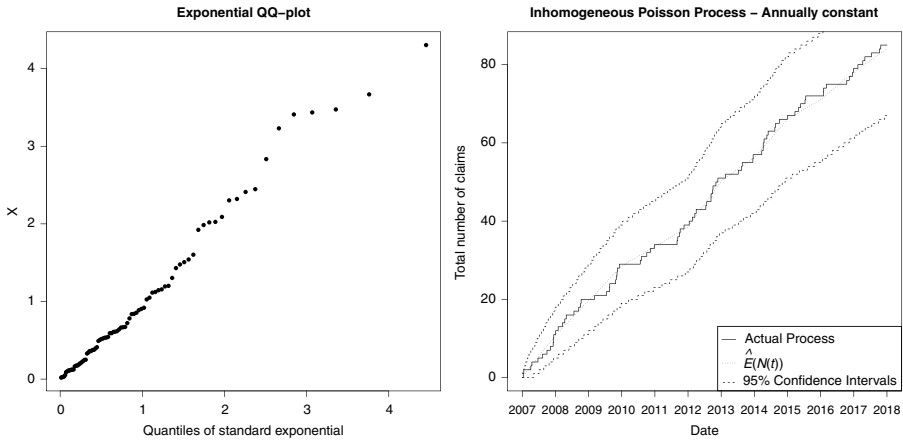
FIGURE 4: QQ-plot of the standardized inter-arrival times after time change (left) and simulated 95% confidence intervals for an inhomogeneous Poisson process with $\lambda(t)$ estimated as the annual average and observed cumulative count claims (right).

3.2. Severity modeling

3.2.1. *Statistical analysis for ultimates.*

Given that the data correspond to the largest marine liability claims (above US $2.85 million), one can expect them to be heavy-tailed. We examine the fit of four different distributions: exponential, Weibull, log-normal, and Pareto, to the ultimate values of the 85 combined claims (for the closed claims, these coincide with the final paid amounts), cf. Albrecher *et al.* (2017, Chapter 4). Figure 5 depicts the resulting QQ-plots, which show convex shapes for the exponential, log-normal, and Weibull case, clearly indicating that the tail of the data set is heavier than the tail of these distributions. In the Pareto QQ-plot, one observes a linear pattern indicating that the Pareto distribution can be a good model for the severity. This is also supported by the mean excess plot in Figure 6 which shows an increasing linear behavior.

All this indicates that extreme value analysis should be used to further explore the claims. In particular, we expect the extreme value index (EVI) γ to be positive, such that one is in the *Fréchet* domain of attraction, see for example Albrecher *et al.* (2017), McNeil (1997).

The most popular estimator of γ in this case is the Hill estimator (1975)

$$H_{k,n} = \frac{1}{k} \sum_{j=1}^{k} \ln \left(X_{n-j+1,n} \right) - \ln \left(X_{n-k,n} \right),$$

where n is the sample size, $X_{n-k,n}$ is the $(k+1)$-largest value in the sample, and k is the number of largest observations used in the estimation. The Hill estimator can be interpreted as an estimator of the slope of a strict Pareto QQ-plot or as the MLE of the parameter $1/\alpha$ based on the strict Pareto distribution given by
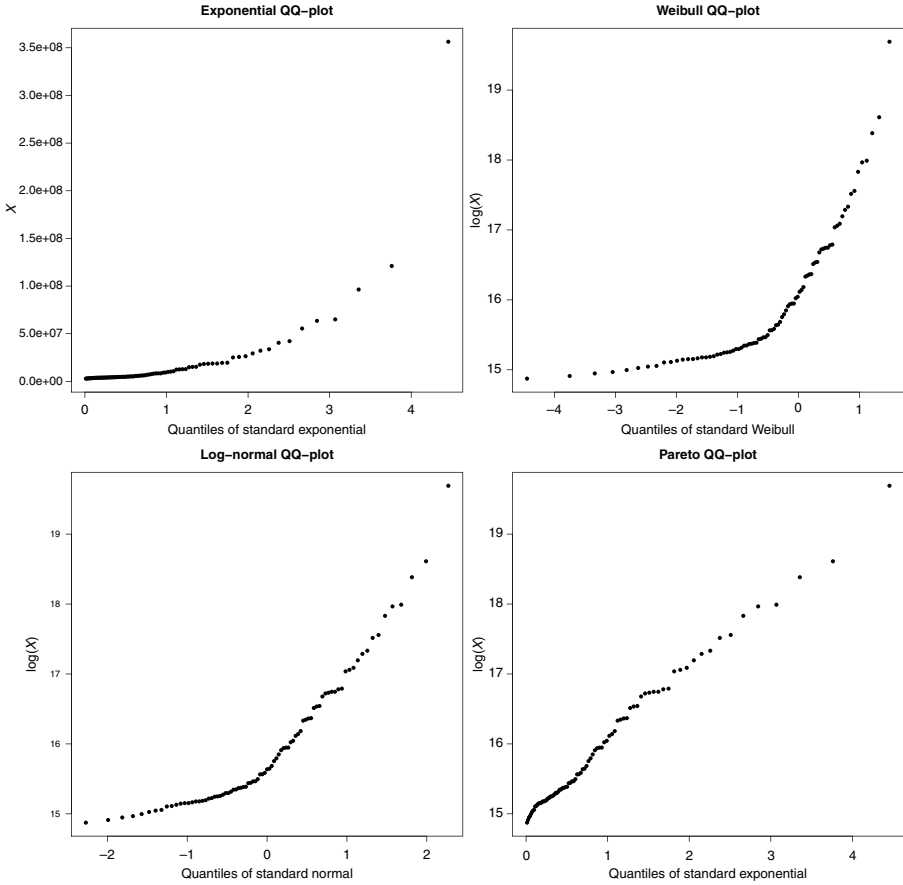
FIGURE 5: QQ-plots for the ultimate values of the combined claims in excess of US $2.85 million.

$$F(x) = 1 - \left(\frac{t}{x}\right)^{\alpha}, \qquad x > t, \tag{3.3}$$

when using the *Peak over Threshold* (POT) approach applied to the values $Y = X/t$ conditional on $X > t$ for a large t. If the actual tail is not strict Pareto, this estimator for γ will be biased. One, therefore, often considers alternative estimators. Among them are a biased-reduced Hill estimator designed for distributions in the Hall class (cf. Hall, 1982) and a MLE using the POT approach based in this case on the extended Pareto distribution (EPD)

$$G_{\gamma,\delta,\tau}(x) = 1 - (x(1 + \delta - \delta x^{\tau}))^{-1/\gamma}, \qquad x > 1, \tau < 0, \delta > \max{(-1, 1/\tau)},$$

(see e.g., Albrecher *et al.*, 2017 for details on all these estimators). Figure 7 presents the Hill, the bias-reduced Hill, and the EPD estimates as a function of k. The Hill plot exhibits a rather stable behavior, indicating an EVI around 1. This evidences a heavy tail with even possibly infinite mean. The bias-reduced
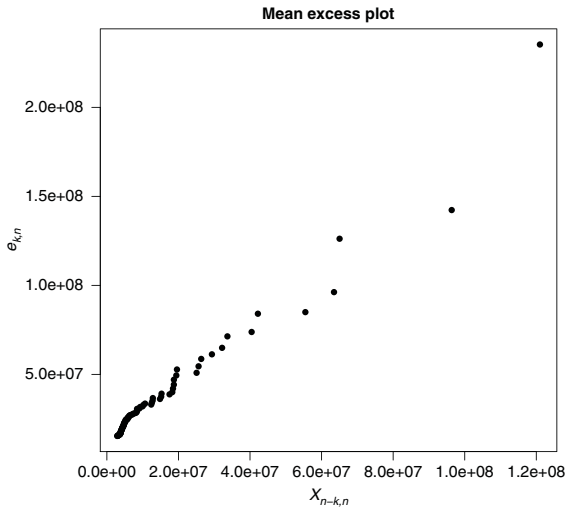
Mean excess plot

FIGURE 6: Empirical mean excess function for the ultimate values of the combined claims in excess of US $2.85 million.
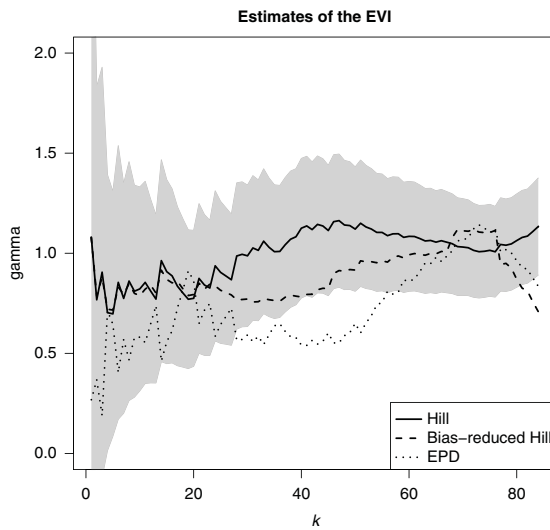
Estimates of the EVI

FIGURE 7: Hill (together with a 95% confidence interval), bias-reduced Hill, and EPD estimator as a function of k.

Hill estimator shows no bias when only the largest claims are considered, $k \in (1, 25)$, while for larger values of k it evidences a slight positive bias on the Hill estimates. The EPD estimator shows smaller values of the EVI around 0.7.

We also add an estimation of the EVI that would allow for nonpositive γ values as well. The slope of the generalized QQ-plot ($\log\left(\frac{n+1}{k+1}\right)$, $\log\left(X_{n-k,n}H_{k,n}\right)$), $k = 1, \dots, n-1$ generalizes the Hill estimator to
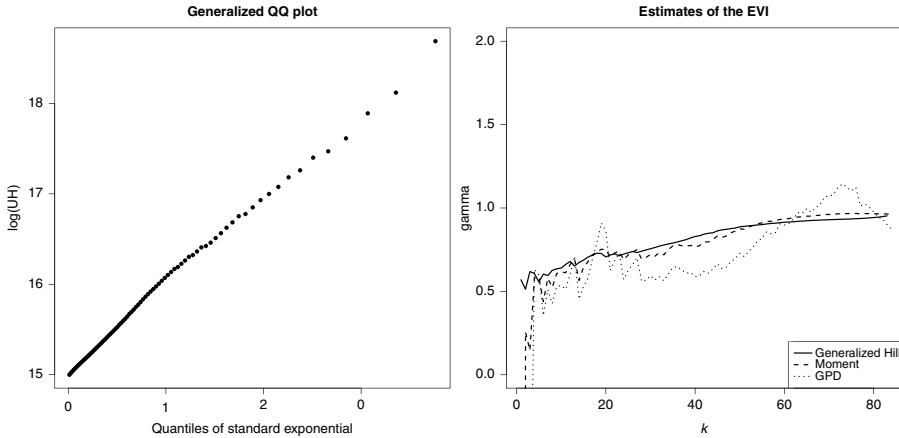
FIGURE 8: Generalized QQ-plot (left), generalized Hill, moment, and GPD estimates as a function of k (right).

$$\hat{\gamma}_{k,n}^{GH} = \frac{1}{k} \sum_{j=1}^{k} \ln\left(X_{n-j,n} H_{j,n}\right) - \ln\left(X_{n-k-1,n} H_{k+1,n}\right).$$

Another generalization of the Hill estimator is the moment estimator (Dekkers *et al.*, 1989)

$$\hat{\gamma}_{k,n}^{M} = H_{k,n} + 1 - \frac{1}{2}\left(1 - \frac{H_{k,n}^2}{H_{k,n}^{(2)}}\right)^{-1}, \qquad \text{with}$$

$$H_{k,n}^{(2)} = \frac{1}{k} \sum_{j=1}^{k} \left(\ln\left(X_{n-j+1,n}\right) - \ln\left(X_{n-k,n}\right)\right)^2.$$

Assuming that the limiting distribution of the values $Y = X - t$ conditional on $X > t$ for large t is a generalized Pareto distribution (GPD) with c.d.f. $G_{\gamma,\tau}(x) = 1 - (1 + \tau x)^{-1/\gamma}$, $1 + \tau x > 0$, one gets by MLE a real-valued POT estimate of γ. Figure 8 shows the generalized QQ-plot that exhibits an increasing linear pattern with a positive slope again suggesting a distribution in the *Fréchet* domain of attraction and confirming the heavy tail nature of the data. The right-hand side of the figure contains the generalized Hill, the moment, and the GPD estimates as a function of k, all suggesting a stable behavior and supporting a positive value of the EVI between 0.6 and 0.95, slightly smaller than the Hill estimates and around the same value as the bias-reduced Hill and the EPD estimates.

3.2.2. *Statistical analysis with censoring.*
As it is not uncommon in the industry, in the previous section, the ultimates for the claims were treated as if they were the final values. We now would like
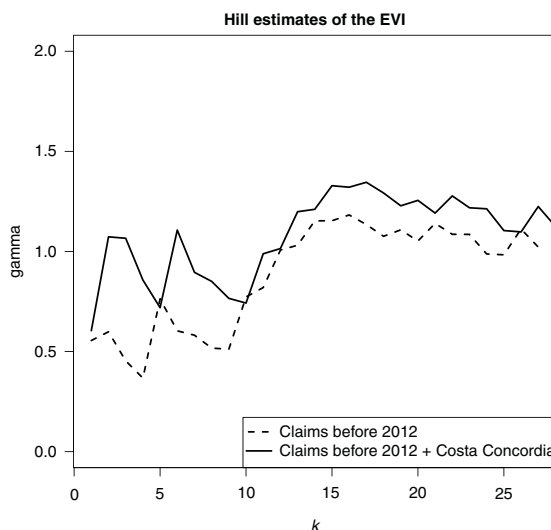
FIGURE 9: Hill estimator adapted for interval censoring, with cumulative paid amounts as lower bounds and incurred as upper bounds for claims occurred before 2012 and with Costa Concordia claim added.

to take into account the fact that most of the claims are still open and their final value is not known yet. Concretely, we examine the estimates of the EVI of the combined claims under interval censoring for the open claims with a lower truncation point given by the reporting threshold of US $2.85 million and a lower bound given by the cumulative amounts already paid. In addition, we apply two methods used in Albrecher *et al.* (2017, p. 107) to specify upper bounds for the censored claims.

In the first method, the incurred values are used as upper bounds for the claims with at least 8 years of development (39 claims occurred before 2012, 26 of them open). The number eight is chosen because the incurred values, after reaching the 8 years of development, turn out to be an actual upper bound of the final payments for all the closed claims. Figure 9 presents the Hill estimator adapted for interval censoring using this first method (see e.g., Albrecher *et al.*, 2017 for details). One identifies two levels of the EVI, around 1.1 for $k > 12$ and around 0.6 for $k \in (1, 10)$. The lower level of the EVI indicates a less heavy tail when compared to the estimators without censoring. However, this reduction of the EVI may be rather due to the exclusion of the most expensive claim (Costa Concordia), which occurred in January 2012. In fact, if the latter is added to the previous 39 claims in the analysis, the level of the EVI goes up again substantially (cf. Figure 9). This highlights the extreme nature of the Costa Concordia loss, which is by a factor three bigger than the second-largest loss in the data set and still should not be assumed to be an outlier.

The second method for interval censoring proposed in Albrecher *et al.* (2017) computes for each claim i the ratios $R_{i,d}$ of the final cumulative paid amount (registered in 2018) over the incurred value for each development year
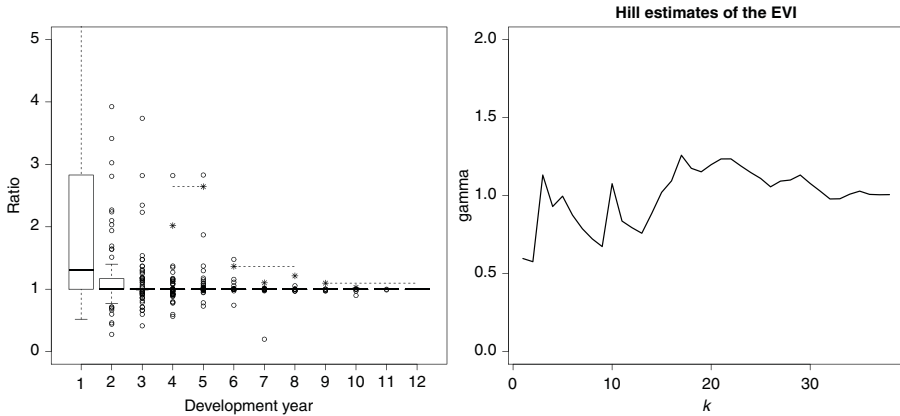
FIGURE 10: Boxplots of the ratios $R_{i,d}$ for $d = 1, 2, \ldots, 12$ and right endpoints estimates (left). The final factors used to multiply the incurred values by development year are shown as dashed lines. Hill estimator adapted for interval censoring, with cumulative paid amounts as lower bounds and incurred multiplied by factor as upper bounds for claims occurred before 2016 (right).

d. If the ratio $R_{i,d}$ is larger than 1, the incurred value in development year d is smaller than the latest available paid amount. Thus, $R_{i,d}$ gives the factor by which we would have to multiply the incurred value to be a reliable upper bound. The ratio is also right-censored if the claim i is still open, thus the right endpoints of $R_{i,d}$ are estimated per development year d using the 99.9% quantile corrected by censoring as described in Einmahl *et al.* (2008). Figure 10 (left) shows the boxplots of $R_{i,d}$ and the estimated right endpoints using the quantiles corrected by censoring, by development year. The estimated endpoints of $R_{i,d}$ of claims with three or less years of development are still not reliable, so only claims occurred before 2016 (72 claims, 48 of them open) are used in this case. These estimates are not strictly decreasing for higher development years as one would initially expect; therefore, we adopt a conservative approach using the estimate of development year 5 (2.64) also for development year 4, the estimate of development year 6 (1.37) also for development years 7 and 8, and the estimate of development year 9 (1.1) also for development years 10, 11, and 12. These incurred values scaled by the former factors are used as an upper bound for the censored claims. The upper bounds obtained by this approach are higher than the ultimate values for all open claims, except three claims for which the values are at least 96% the amount of the ultimates. Figure 10 (right) presents the Hill estimates adapted for censoring under the second method. We can see that in this case the EVI takes again values around 1.

Hence, taking into account the censored nature of data points indicates a value of γ around 1 or even pointing toward an infinite mean of the underlying marine liability risk.

3.2.3. *Statistical analysis of stationarity.*

So far, we assumed that the severity distribution is stationary over time. However, as mentioned in Section 2, it is expected that marine liability claims become more expensive over the years. Hence, we apply the tests T_3 and T_4
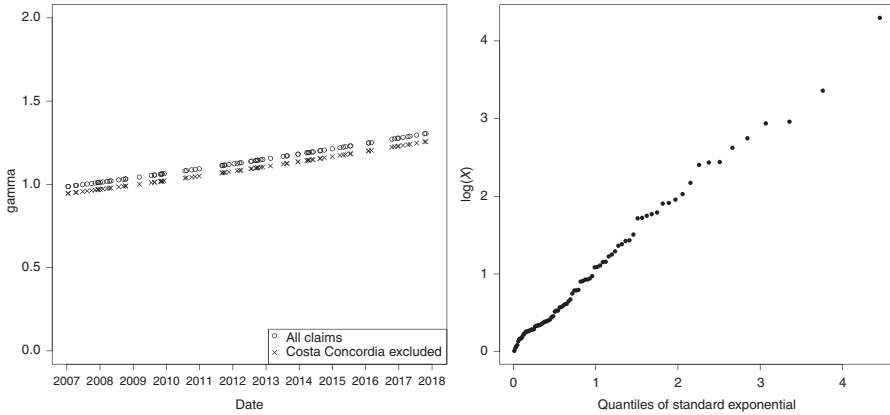
FIGURE 11: Estimated EVI $\hat{\gamma}_i$ as a function of time assuming Pareto claims (left) and Pareto QQ-plot of $(X_i/M)^{1/\hat{\gamma}_i}$ (right).

recently derived in Einmahl *et al.* (2016) for the hypothesis that the EVI is constant over time, in the heavy-tailed case ($\gamma > 0$). In this case, $n = 85$ and we take $k = 25$ given that it is one of the first values after which the Hill plot stabilizes; tests T_3 (with $\delta = \frac{1}{4}$) and T_4 (with $m = 4$) produce p-values equal to 0.32 and 0.55, respectively. Therefore, on the basis of these tests and the available data, one would not reject the null hypothesis of a constant EVI over time.

Alternatively, one can try to fit a time regression for the EVI of the form

$$\gamma_i = \exp\left(\beta_0 + \beta_1 T_i\right), \quad i = 1, \ldots, n,$$

assuming that the claims follow a Pareto distribution (see e.g., Beirlant and Goegebeur, 2003). The MLEs of the parameters equal $\hat{\beta}_0 = -0.0139$ and $\hat{\beta}_1 = 0.00007$, respectively. The positive value of the parameter β_1 indicates that the EVI of the data set, and hence the heaviness of the tail, increases over time. Fitting the regression without the Costa Concordia loss yields $\hat{\beta}_0^* = -0.0566$ and $\hat{\beta}_1^* = 0.00007$. The value of the parameter β_1 remains unchanged evidencing the same trend toward heavier claims over time still remains in the absence of the most expensive claim, so the result is not an artifact of that one huge claim. Figure 11 (left) shows the predicted values $\hat{\gamma}_i$ when using the estimated parameters above, under the two cases with all data and also without Costa Concordia. We note that the EVI rises from 0.95 at the beginning of the observed period up to more than 1.3 at the end; evidencing a significant increment in the value of this parameter. Figure 11 (right) presents the Pareto QQ-plot of the amounts $(X_i/M)^{1/\hat{\gamma}_i}$ which should be Pareto with tail index 1 if the regression model is appropriate. This graph indicates a good fit of the regression model, improving the pattern obtained for a constant EVI is considered (cf. Figure 5 bottom right).

To summarize, we note that the EVI for this set of marine liability claim amounts behaves consistently when bias and interval censoring corrections of the Hill estimator are considered. The EVI seems to be located between 0.7

and 1.15, giving clear evidence of the heavy-tailed nature of the claims for this line of business, suggesting that the underlying variance is infinite and even the underlying mean could possibly be infinite. One also saw that conclusions are quite sensitive to the statistical method used: while the tests according to Einmahl *et al.* (2016) would not significantly reject stationarity over time, the regression approach of Beirlant and Goegebeur (2003) does indicate the (intuitively expected) increase in the heaviness of the tail over time in a rather convincing manner.

It is worthwhile to mention that in addition to the heavy-tailed nature of the claims, one should also consider the effect of the accumulation and increase in insured values and forthcoming changes in regulation and law, to properly model future marine liability exposures.

4. MARKET EXCESS OF LOSS PROGRAM FOR EXTREME LOSSES

Let us now consider an insurance market with an *XL reinsurance program* designed to cover the most extreme claims appearing in the market. This is indeed the case for the marine liability insurance market, where since 1951 the IGP&I manages the IG GXL Reinsurance Contract (for many years, the world's largest reinsurance contract), to cover the highest liability losses to which the marine industry is exposed. The structure of this contract is complex and changes every year.[1] Its retention has continuously increased during recent years, passing from US $50 million in 2010 to US $100 million in 2019, cf. IGP&I (2017). The losses above the IG GXL retention are covered in four layers that are reinsured in the open market by dozens of insurers and reinsurers that take different shares in each layer (according to IGP&I, 2015, 91 reinsurers worldwide participated in the contract in 2014). Some then opt to facultatively retrocede part of their assumed exposure in order to reduce single event exposures. It is worth noting that this type of reinsurance program also appears in other markets, for instance, flood insurance in the United States, where the Federal Emergency Management Agency underwrites the National Flood Insurance Program's Reinsurance Program (in which 28 reinsurers participated in 2019) to cover flood claims in excess of US $4 billion.[2] According to the design of such a reinsurance program, the expected annual number of claims to be covered is scarce while its severity is major.

Assume that the *market XL reinsurance program* has H different layers, of size L_h for $h = 1, \ldots, H$, in excess of a retention M, that is,

$$\text{1st layer:} \quad L_1 \ \text{xs} \ M,$$

$$\vdots \qquad\qquad \vdots$$

$$h\text{th layer:} \quad L_h \ \text{xs} \ (M + L_1 + L_2 + \cdots + L_{h-1}),$$

$$\vdots \qquad\qquad \vdots$$

$$H\text{th layer:} \quad L_H \ \text{xs} \ (M + L_1 + L_2 + \cdots + L_{H-1}).$$

Generally, $L_H < \infty$, so the part of the losses in excess of $M + \sum_{h=1}^{H} L_h$ (usually a very large value) is not covered by the program. If $L_H = \infty$, the program provides unlimited coverage for every claim. To simplify notation, we denote by $K_h := L_1 + \cdots + L_h$ the cumulative sum of the layers for $h = 1, \ldots, H$ and define $K_0 := 0$.

Let the random variable N denotes the number of losses in the insurance market above the threshold $M > 0$ and let the random variables X_i, $i = 1, \ldots, N$ denote the size of these losses, which for the rest of the paper we assume to be independent and identically distributed with c.d.f. F_X, and N and X_i being independent. The aggregate value of the losses then is

$$S = \sum_{i=1}^{N} X_i.$$

Due to the large size of the reinsurance program, several insurance and reinsurance companies take parts in its different layers. We consider a reinsurer r that participates in the different layers of the market reinsurance program, as well as in the XL contracts of C different cedents which also participate in the program.

Remark 1. *In order to avoid confusion, from here on, we use the term* program *to refer to the market XL reinsurance program and the term* contract *for the XL contracts that the reinsurer r has with the C cedents. In marine liability insurance, the cedents regularly comprise Lloyd's syndicates, giving the important role of the London Market in this line of business, while reinsurer r is typically a global reinsurer.*

Let δ_c^h denote the proportion of participation of cedent c ($c = 1, \ldots, C$), in layer h of the program. Then, the gross amount of each single loss X_i in excess of M taken by the cedent c is given by

$$X_{c,i} = \sum_{h=1}^{H} \delta_c^h \left[(X_i - (M + K_{h-1}))_+ \wedge L_h \right]$$

$$= \sum_{h=1}^{H} \delta_c^h \left[(X_i \wedge (M + K_h)) - (X_i \wedge (M + K_{h-1})) \right], \qquad (4.1)$$

where $X \wedge u := \min\{X, u\}$, $(X - u)_+ := \max\{X - u, 0\}$, and the maximum gross amount per single loss for cedent c is equal to $\sum_{h=1}^{H} \delta_c^h L_h$.

The cedents also underwrite XL contracts to reduce the impact of single extreme claims. These contracts are reinsured by several companies in the market, among them the reinsurer r, who takes a share $\Delta_c \in [0, 1]$ on the $u_c M$ xs $d_c M$ contract of cedent c, for some $u_c, d_c > 0$. Then for each single loss X_i covered by the program, the participation of the reinsurer r due to the portion he has to pay for the contract with cedent c is given by

$$
\begin{aligned}
X_{r,c,i} &= \Delta_c \left[(X_{c,i} - d_c M)_+ \wedge u_c M \right] \\
&= \Delta_c \left\{ [X_{c,i} \wedge (d_c + u_c)M] - [X_{c,i} \wedge d_c M] \right\} \\
&= \Delta_c \left\{ \left[\left(\sum_{h=1}^{H} \delta_c^h [(X_i \wedge (M + K_h)) - (X_i \wedge (M + K_{h-1}))] \right) \wedge (d_c + u_c)M \right] \right. \\
&\quad\quad \left. - \left[\left(\sum_{h=1}^{H} \delta_c^h [(X_i \wedge (M + K_h)) - (X_i \wedge (M + K_{h-1}))] \right) \wedge d_c M \right] \right\} \\
&= \Delta_c \sum_{h=1}^{H} \delta_c^h \left[\left(X_i \wedge k_{c,2}^h \right) - \left(X_i \wedge k_{c,1}^h \right) \right], \qu\quad\quad\quad\quad\quad\quad\quad (4.2)
\end{aligned}
$$

with

$$
\begin{aligned}
k_{c,1}^h &= \min \left\{ \max \left\{ M + K_{h-1}, \ M + K_{h-1} + \frac{d_c M - \delta_c^1 L_1 - \cdots - \delta_c^{h-1} L_{h-1}}{\delta_c^h} \right\}, \right. \\
&\quad\quad\quad \left. M + K_h \right\}, \\
k_{c,2}^h &= \max \left\{ \min \left\{ M + K_h, \ M + K_{h-1} + \frac{(d_c + u_c)M - \delta_c^1 L_1 - \cdots - \delta_c^{h-1} L_{h-1}}{\delta_c^h} \right\}, \right. \\
&\quad\quad\quad \left. M + K_{h-1} \right\},
\end{aligned}
$$

From the above, we must require that $\sum_{h=1}^{H} \delta_c^h L_h > d_c M$, otherwise $X_{r,c,i} = 0$ and the cedent contract does not transfer any risk. In fact, from the point of view of cedent c, it makes sense to have the XL contract such that $(d_c + u_c)M \le \sum_{h=1}^{H} \delta_c^h L_h$, that is the retention plus the limit being smaller than its maximum gross loss.

   If the reinsurer participates in the reinsurance contracts of C different cedents and also takes direct participation δ_r^h in the program layer h, then for each loss X_i covered by the program the amount he has to pay equals $X_{r,i} + \sum_{c=1}^{C} X_{r,c,i}$. Here $X_{r,i}$ is given by (4.1) with δ_c^h replaced by δ_r^h and $X_{c,i}$ replaced by $X_{r,i}$, and $X_{r,c,i}$ is given by (4.2). The total annual loss for reinsurer r then is

$$
S_R = \sum_{i=1}^{N} \left[\sum_{c=1}^{C} X_{r,c,i} + X_{r,i} \right] := \sum_{i=1}^{N} X_{R,i} := \sum_{c=1}^{C} S_{r,c} + S_r, \quad\quad (4.3)
$$

where

$$
X_{R,i} = \sum_{c=1}^{C} X_{r,c,i} + X_{r,i} \quad\quad\quad\quad\quad\quad\quad (4.4)
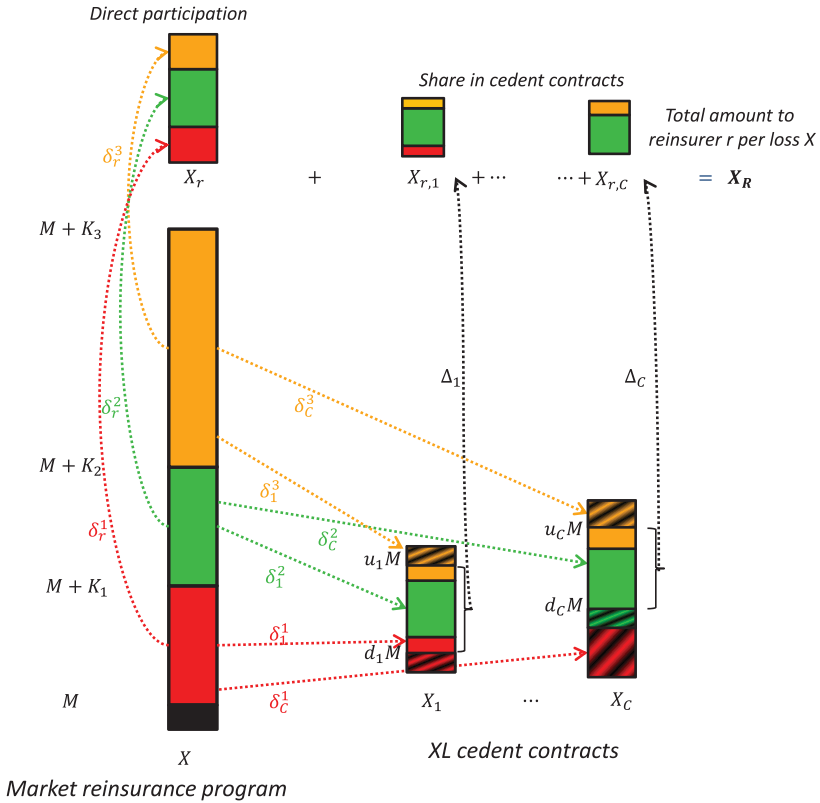$$

FIGURE 12: Reinsurer r participation in claim X covered under the market reinsurance program ($H = 3$).

denotes the total amount that the reinsurer r has to pay for a single loss X_i (from its direct participations and the contracts with the cedents),

$$S_{r,c} = \sum_{i=1}^{N} X_{r,c,i} \tag{4.5}$$

is the total annual loss the reinsurer has to pay from the contract with cedent c and

$$S_r = \sum_{i=1}^{N} X_{r,i} \tag{4.6}$$

is the total annual loss the reinsurer has to pay from his direct participations in the reinsurance program.

Figure 12 illustrates the participations of reinsurer r in each single loss X_i covered under the *market XL reinsurance program*.

5. Optimization of the Reinsurer Participations in the Market Program

5.1. Principles of premium calculation

Classical principles of premium calculation are based on the idea that the actuarial premium $\Pi[X]$ for a risk X should be equal to the expected loss of the covered risk $\mathbb{E}[X]$ plus a safety loading, see for example, Kaas *et al.* (2008) for an extensive review. As is quite common in the market, in the following, we base our considerations on the expected value principle and the variance principle:

Expected value principle: For some $\theta \geq 0$,

$$\Pi[X] = (1 + \theta)\mathbb{E}[X], \tag{5.1}$$

or

Variance principle: For some $\beta \geq 0$,

$$\Pi[X] = \mathbb{E}[X] + \beta \operatorname{Var}[X]. \tag{5.2}$$

5.2. Risk tolerance limits based on exceedance probabilities

Although top-tier reinsurers have well-diversified portfolios, they are required to control the total accumulation risk originating from extreme events in specific insurance markets. One way to do this is to define risk tolerance limits that the extreme losses cannot surpass on specific (long) return periods. For a general discussion on calibrating risk appetite in insurance, see for example, GIRO (2011). Given the catastrophic nature of the extreme losses covered by the reinsurance program described in Section 4, the risk tolerance limits can be based on a metric widely used in catastrophe modeling, the occurrence exceedance probability (OEP), (see e.g., Mitchell-Wallace *et al.*, 2017). This is defined as the probability that at least one loss exceeds t, that is,

$$\operatorname{OEP}_{N,X}(t) := \mathbb{P}[\max\{X_1, \ldots, X_N\} > t].$$

The reinsurer then typically fixes a set of J risk tolerance limits $t_1 < \cdots < t_J$ for specified probabilities $p_1 > \cdots > p_J$; the concrete values of the risk tolerance limits and corresponding probabilities depend on the available capital, risk appetite, and underwriting strategy of the reinsurer. Under the i.i.d. assumption on the losses X_i, we then have the constraint that the OEP of t_j occurs with a probability smaller than p_j equal to

$$1 - p_j \leq \mathbb{P}[\max\{X_1, \ldots, X_N\} \leq t_j] = \mathbb{E}_N\left[\prod_{i=1}^{N} F_{X_i}(t_j)\right] = \mathbb{E}_N\left[\left(F_X(t_j)\right)^N\right],$$

so that $P_N^{-1}(1-p_j) \le F_X(t_j), j = 1, \ldots, J,$ where $P_N(z) = \mathbb{E}_N\left[z^N\right]$ is the probability-generating function of N.

5.3. Profit optimization under risk tolerance limits for extreme losses

We now consider the optimization problem to identify the participation levels $\delta_r^h, \ h = 1, \ldots, H$ in the layers and $\Delta_c, \ c = 1 \ldots, C$ in the XL contracts with the cedents that maximize the expected annual profit of the reinsurer r. We consider a profit given by premiums minus expected losses, subject to the set of J risk tolerance limits $\text{OEP}_{N,X_R}(t_j) \le p_j, \ j = 1, \ldots, J$ on the aggregate risk of the portfolio. Upper participation limits of reinsurer r in the cedents' contracts and the program layers are denoted by Δ^{UP} and $\delta^{h,UP}, \ h = 1, \ldots, H$. These limits are in practice determined by various factors, for example, whether reinsurer r is a leading or a following reinsurer, how many companies take part in the reinsurance program and how competitive the specific insurance market is. The constrained optimization problem is then given by

$$\max_{\Delta_c, \delta_r^h} \ \Pi[S_r] + \sum_{c=1}^{C} \Pi[S_{r,c}] - \left(\mathbb{E}[S_r] + \sum_{c=1}^{C} \mathbb{E}[S_{r,c}]\right), \ c = 1, \ldots C, \ h = 1, \ldots H,$$

(5.3)

subject to $\quad P_N^{-1}(1-p_1) \le F_{X_R}(t_1),$

$$\vdots$$

$$P_N^{-1}(1-p_J) \le F_{X_R}(t_J),$$

$$\Delta_c \in \left[0, \Delta^{UP}\right], \delta_r^h \in \left[0, \min\left\{\delta^{h,UP}, 1 - \sum_{c=1}^{C} \delta_c^h\right\}\right).$$

Remark 2. *Note that the participations in the contracts with each cedent c and in the program are priced separately through $\Pi[S_{r,c}]$ and $\Pi[S_r]$, as defined in (4.5) and (4.6). In practice, the marine liability portfolio of cedent c is typically composed of its participation in the IGP&I reinsurance program together with another independent and less extreme marine liability business. Such independent business must be added inside the calculation of the premium $\Pi[S_{r,c}]$. However, for simplicity, we consider here that the reinsurance contract with each cedent only involves the cedent's participation in the IGP&I program. The risk tolerance constraints are fixed on the aggregate losses of the portfolio S_R as defined in (4.3) with frequency N and severity X_R given by (4.4).*

Remark 3. *In practice, the reinsurance program and the contracts with the cedents are priced at different dates. In marine liability, the IG GXL reinsurance program is in force every year on February 20th,[3] while most contracts with commercial (re)insurers are renewed on January 1st, April 1st, or July 1st. The optimization problem in (5.3) can be of particular interest for the underwriting team of reinsurer r, who can evaluate before the start of an underwriting year*

which would be the optimal participations needed in the reinsurance program and cedent contracts, based on their structure in the previous year, the anticipated modifications, and the risk tolerance limits on the OEP according to the strategy of the company.

It is important to note that if $L_H < \infty$, the random variable X_R cannot exceed

$$M_R = \sum_{c=1}^{C} \left[\Delta_c \sum_{h=1}^{H} \delta_c^h \left[k_{c,2}^h - k_{c,1}^h \right] \right] + \sum_{h=1}^{H} \delta_r^h L_h,$$

with $\mathbb{P}[X_R = M_R] = 1 - F_X (M + K_H)$. We then have for the constraint with the smallest probability p_J that

$$F_X (M + K_H) \leq P_N^{-1}(1 - p_J), \tag{5.4}$$

and additional constraints with smaller probabilities p_j would be irrelevant. The constraints in the optimization problem can be expressed as linear inequalities of Δ_c and δ_r^h, such that for $\tau_j := F_X^{-1} \left(P_N^{-1}(1 - p_j) \right)$

$$P_N^{-1}(1 - p_j) \leq F_{X_R}(t_j),$$

$$P_N^{-1}(1 - p_j) \leq \mathbb{P}\left[\sum_{h=1}^{H} \left\{ \sum_{c=1}^{C} \Delta_c \delta_c^h \left[\left(X \wedge k_{c,2}^h \right) - \left(X \wedge k_{c,1}^h \right) \right] + \delta_r^h \left[(X \wedge (M + K_h)) \right. \right. \right.$$

$$\left. \left. \left. - (X \wedge (M + K_{h-1})) \right] \right\} \leq t_j \right],$$

$$\sum_{h=1}^{H} \left\{ \sum_{c=1}^{C} \Delta_c \delta_c^h \left[\left(\tau_j \wedge k_{c,2}^h \right) - \left(\tau_j \wedge k_{c,1}^h \right) \right] + \delta_r^h \left[\left(\tau_j \wedge (M + K_h) \right) \right. \right.$$

$$\left. \left. - \left(\tau_j \wedge (M + K_{h-1}) \right) \right] \right\} \leq t_j.$$

5.4. Profit optimization using the expected value principle

If the reinsurer uses the expected value principle (5.1) to price the contracts he has with the cedents and its participation in the reinsurance program, the objective function of the optimization problem (5.3) becomes

$$\Pi[S_r] + \sum_{c=1}^{C} \Pi[S_{r,c}] - \left(\mathbb{E}[S_r] + \sum_{c=1}^{C} \mathbb{E}[S_{r,c}] \right)$$

$$= (1 + \theta_r)\mathbb{E}[S_r] + \sum_{c=1}^{C} (1 + \theta_c)\mathbb{E}[S_{r,c}] - \left(\mathbb{E}[S_r] + \sum_{c=1}^{C} \mathbb{E}[S_{r,c}] \right)$$

$$= \theta_r \mathbb{E}[S_r] + \sum_{c=1}^{C} \theta_c \mathbb{E}[S_{r,c}], \quad c = 1, \dots C, \quad h = 1, \dots H.$$

That is, the optimization problem in (5.3) is then a linear program on the variables Δ_c and δ_r^h for $c = 1, \ldots, C$, $h = 1, \ldots, H$. For the general theory on linear programming, we refer to Vanderbei (2014) and Luenberger and Ye (2008). The optimization problem in standard form has $C + H$ decision variables and $J + C + H$ constraints of the generic form

$$\max_{\delta} \quad \mathbf{c}\delta^T$$
$$\text{subject to} \quad \mathbf{A}\delta^T \leq \mathbf{b}^T,$$
$$\delta \geq \mathbf{0},$$

where

$$\delta = \left(\delta_r^1, \ldots, \delta_r^H, \Delta_1, \ldots, \Delta_C\right), \tag{5.5}$$

$$\mathbf{c} = \left(c_1, \ldots, c_H, c_{H+1}, \ldots, c_{H+C}\right), \tag{5.6}$$

$$\mathbf{A} = \begin{pmatrix} a_{1,1} & \cdots & \cdots & a_{1,H+C} \\ \vdots & \ddots & & \vdots \\ a_{J,1} & \cdots & \cdots & a_{J,H+C} \\ 1 & 0 & \cdots & 0 \\ 0 & \ddots & & \vdots \\ \vdots & & 1 & 0 \\ 0 & \cdots & 0 & 1 \end{pmatrix}, \tag{5.7}$$

$$\mathbf{b} = \left(t_1, \ldots, t_J, \delta^{1,UP} \wedge \left(1 - \sum_{c=1}^{C} \delta_c^1\right), \ldots, \delta^{H,UP} \wedge \left(1 - \sum_{c=1}^{C} \delta_c^H\right), \Delta_1^{UP}, \ldots, \Delta_C^{UP}\right), \tag{5.8}$$

with

$$c_i = \theta_r \mathbb{E}[N] \left[\mathbb{E}[X \wedge (M + K_i)] - \mathbb{E}[X \wedge (M + K_{i-1})]\right], \quad i = 1, \ldots, H,$$

$$c_{H+i} = \theta_i \mathbb{E}[N] \left(\sum_{h=1}^{H} \delta_i^h \left[\mathbb{E}\left[X \wedge k_{i,2}^h\right] - \mathbb{E}\left[X \wedge k_{i,1}^h\right]\right]\right), \quad i = 1, \ldots, C,$$

$$a_{j,i} = \left[\left(\tau_j \wedge (M + K_i)\right) - \left(\tau_j \wedge (M + K_{i-1})\right)\right], \quad j = 1, \ldots, J, \ i = 1, \ldots, H$$

$$a_{j,H+i} = \sum_{h=1}^{H} \delta_i^h \left[\left(\tau_j \wedge k_{i,2}^h\right) - \left(\tau_j \wedge k_{i,1}^h\right)\right], \quad j = 1, \ldots, J, \ i = 1, \ldots, C$$

Note that $\delta = \mathbf{0}$ is always a feasible solution (no participation and no profit). Hence, a solution to this optimization problem always exists. The dual of this program has $J + C + H$ decision variables and $C + H$ constraints and can be formulated as follows:

$$\min_{y} \quad \mathbf{b}y^{\mathbf{T}}$$
$$\text{subject to} \quad y\mathbf{A} \geq \mathbf{c},$$
$$y \geq \mathbf{0},$$

where $\boldsymbol{y} = (y_1, \ldots, y_{J+H+C})$. The dual optimization problem minimizes factors on the risk tolerance constraints, maximum participations on the layers and cedents' reinsurance contracts, subject to the condition that the factors applied to the maximum losses are bigger than the total profit per layer and cedent contract. Depending on the number of factors on each side, the dual formulation of the problem can be simpler than the primal formulation.

5.5. Profit optimization using the variance principle

If the reinsurer uses the variance principle (5.2) to price the contracts with cedents and for the participation in the reinsurance program, the objective function of the optimization problem in (5.3) becomes

$$\Pi[S_r] + \sum_{c=1}^{C} \Pi[S_{r,c}] - \left(\mathbb{E}[S_r] + \sum_{c=1}^{C} \mathbb{E}[S_{r,c}] \right)$$

$$= \mathbb{E}[S_r] + \beta_r \operatorname{Var}[S_r] + \sum_{c=1}^{C} \left(\mathbb{E}[S_{r,c}] + \beta_c \operatorname{Var}[S_{r,c}] \right)$$

$$- \left(\mathbb{E}[S_r] + \sum_{c=1}^{C} \mathbb{E}[S_{r,c}] \right)$$

$$= \beta_r \operatorname{Var}[S_r] + \sum_{c=1}^{C} \beta_c \operatorname{Var}[S_{r,c}], \qquad c = 1, \ldots, C, \quad h = 1, \ldots, H.$$

In this case, the optimization problem (5.3) is a standard quadratic program on the variables Δ_c and δ_r^h for $c = 1, \ldots, C$ and $h = 1, \ldots, H$. It can be expressed with $C + H$ decision variables and $J + C + H$ constraints as follows:

$$\max_{\delta} \quad \delta \mathbf{D} \delta^T$$
$$\text{subject to} \quad \mathbf{A} \delta^T \le \mathbf{b}^T,$$
$$\delta \ge \mathbf{0},$$

with

$$\mathbf{D} = \begin{pmatrix} d_{1,1} & \cdots & d_{1,H} & 0 & \cdots & \cdots & 0 \\ \vdots & \ddots & \vdots & \vdots & \ddots & & \vdots \\ d_{H,1} & \cdots & d_{H,H} & 0 & \cdots & & 0 \\ 0 & \cdots & 0 & d_{H+1,H+1} & 0 & \cdots & 0 \\ \vdots & \ddots & \vdots & 0 & d_{H+2,H+2} & & \vdots \\ \vdots & & \vdots & & \ddots & & \vdots \\ 0 & \cdots & 0 & 0 & \cdots & \cdots & d_{H+C,H+C} \end{pmatrix},$$

and

$$
\begin{aligned}
d_{j,i} = \beta_r \{ & \mathbb{E}[N][\operatorname{Cov}[X \wedge (M + K_i), X \wedge (M + K_j)] \\
& - \operatorname{Cov}[X \wedge (M + K_i), X \wedge (M + K_{j-1})] \\
& - \operatorname{Cov}[X \wedge (M + K_{i-1}), X \wedge (M + K_j)] \\
& + \operatorname{Cov}[X \wedge (M + K_{i-1}), X \wedge (M + K_{j-1})]]] \\
& + \operatorname{Var}[N][\mathbb{E}[X \wedge (M + K_i)]\,\mathbb{E}[X \wedge (M + K_j)] \\
& - \mathbb{E}[X \wedge (M + K_i)]\,\mathbb{E}[X \wedge (M + K_{j-1})] \\
& - \mathbb{E}[X \wedge (M + K_{i-1})]\,\mathbb{E}[X \wedge (M + K_j)] \\
& + \mathbb{E}[X \wedge (M + K_{i-1})]\,\mathbb{E}[X \wedge (M + K_{j-1})]]]\} \\
& j, i = 1, \dots, H
\end{aligned}
$$

$$
\begin{aligned}
d_{H+i, H+i} = \beta_i \Bigg\{ & \mathbb{E}[N]\Bigg[\sum_{h=1}^{H} \sum_{h'=1}^{H} \delta_i^h \delta_i^{h'} \Big[\operatorname{Cov}[X \wedge k_{i,2}^h, X \wedge k_{i,2}^{h'}] - \operatorname{Cov}[X \wedge k_{i,2}^h, X \wedge k_{i,1}^{h'}] \\
& - \operatorname{Cov}[X \wedge k_{i,1}^h, X \wedge k_{i,2}^{h'}] + \operatorname{Cov}[X \wedge k_{i,1}^h, X \wedge k_{i,1}^{h'}]\Big] \Bigg] \\
& + \operatorname{Var}[N]\Bigg[\sum_{h=1}^{H} \sum_{h'=1}^{H} \delta_i^h \delta_i^{h'} \Big[\mathbb{E}[X \wedge k_{i,2}^h]\,\mathbb{E}[X \wedge k_{i,2}^{h'}] - \mathbb{E}[X \wedge k_{i,2}^h]\,\mathbb{E}[X \wedge k_{i,1}^{h'}] \\
& - \mathbb{E}[X \wedge k_{i,1}^h]\,\mathbb{E}[X \wedge k_{i,2}^{h'}] + \mathbb{E}[X \wedge k_{i,1}^h]\,\mathbb{E}[X \wedge k_{i,1}^{h'}]\Big] \Bigg] \Bigg\}, \\
& i = 1, \dots, C,
\end{aligned}
$$

and δ, $\mathbf{A}$, and $\mathbf{b}$ defined as in (5.5), (5.7), and (5.8), respectively. As in Section 5.4, the trivial solution $\delta = \mathbf{0}$ is feasible, so that a solution to this optimization problem always exists.

6. ILLUSTRATION OF THE OPTIMIZATION FOR THE REINSURER PARTICIPATIONS

Let us assume that the frequency and severity distributions above the retention $M = 100$ are given by $N \sim \operatorname{Poisson}(\lambda = 1.5)$ and $X_i \sim \operatorname{Pareto}(\alpha = 1.2, t = 100)$ in (3.3). Additionally, let the reinsurance program have three layers $H = 3$ with $M = 100$, $L_1 = 500$, $L_2 = 500$, and $L_3 = 1000$, which corresponds to the structure of the IGP&I reinsurance program in 2017 without the collective overspill layer. We consider four cedents $C = 4$ with participations in the layers and reinsurance contracts as given in Table 1, which implies the limits on the layers of the reinsurance program as given in Table 2.

TABLE 1

CEDENTS PARTICIPATIONS AND XL CONTRACT LIMITS.

Cedent (c)	δ_c^1	δ_c^2	δ_c^3	$\delta_c^1 L_1 + \delta_c^2 L_2 + \delta_c^3 L_3$	$d_c M$	$u_c M$
1	0.05	0.04	0.03	75	10	60
2	0.01	0.04	0.09	115	20	50
3	0.05	0.00	0.04	65	20	20
4	0.00	0.06	0.00	30	15	15

TABLE 2

CEDENTS LIMITS IN LAYERS.

Cedent (c)	$k_{c,1}^1$	$k_{c,2}^1$	$k_{c,1}^2$	$k_{c,2}^2$	$k_{c,1}^3$	$k_{c,2}^3$	$\sum_{h=1}^H \delta_c^h \left(k_{c,2}^h - k_{c,1}^h\right)$
1	300	600	600	1100	1100	1933	60
2	600	600	975	1100	1100	1600	50
3	500	600	600	1100	1100	1475	20
4	600	600	850	1100	1100	2100	15

Additionally, consider that the reinsurer fixes OEP constraints determined by $t_1 = 50$, $t_2 = 75$, $t_3 = 250$, $p_1 = 0.1$, $p_2 = 0.04$, and $p_3 = 0.01$ and the maximum participations in the layers are $\delta^{1,UP} = 0.055$, $\delta^{2,UP} = 0.085$, and $\delta^{3,UP} = 0.1$ and for the cedents $\Delta^{UP} = 0.5$. These values of $\delta^{h,UP}$ correspond to 10% of the available market share for commercial insurers on the corresponding layers of the IGP&I program in 2017. The results of the respective optimization problem under the expected value principle are given below.

Assume initially the same safety loading for the layers of the reinsurance program and the cedents $\theta_r = \theta_1 = \theta_2 = \theta_3 = \theta_4 = 0.2$. Then, we have

$$\mathbf{c} = (45.18, 11.97, 11.26, 1.56, 0.69, 0.41, 0.29),$$

$$\mathbf{A} = \begin{pmatrix} 500 & 314.49 & 0 & 27.58 & 0 & 5 & 3.87 \\ 500 & 500 & 915.26 & 60 & 50 & 20 & 15 \\ 500 & 500 & 1000 & 60 & 50 & 20 & 15 \\ 1 & 0 & \cdots & & & \cdots & 0 \\ 0 & \ddots & & & & & \vdots \\ \vdots & & & & & & 0 \\ 0 & \cdots & & & & \cdots & 0 & 1 \end{pmatrix},$$

$$\mathbf{b} = (50, 75, 250, 0.055, 0.085, 0.1, 0.5, 0.5, 0.5, 0.5).$$

The linear program can, for example, be solved with the classical simplex method developed by Dantzig (1951). In this case, the optimal solution is a profit of 3.659 with the following parameters:

$$(\delta_r^{1*}, \delta_r^{2*}, \delta_r^{3*}, \Delta_1^*, \Delta_2^*, \Delta_3^*, \Delta_4^*) = (0.055, 0.023, 0, 0.5, 0, 0.303, 0).$$
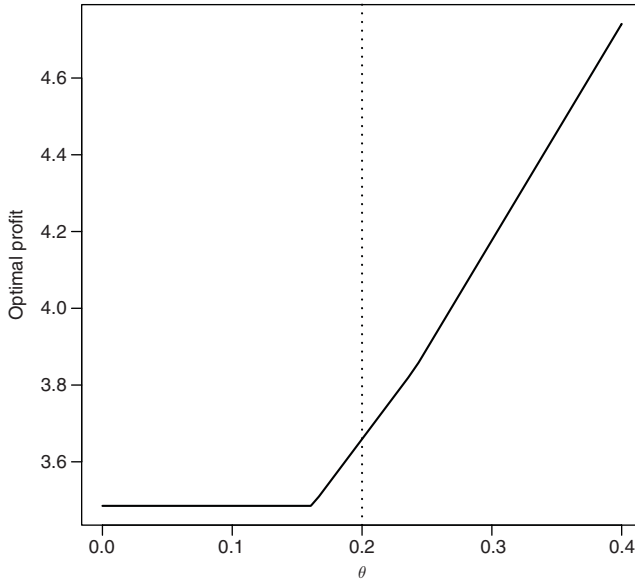
FIGURE 13: Optimal profit as function of θ for $\theta_r = 0.2$.

From the formulation of vector **c** in (5.6), it is clear that the optimal solution does not change for different safety loadings as long as they remain the same for all cedents and the constraints are equal, only the optimal profit will change proportionally to the change in the safety loading. However, we can study the change of the solution if the same safety loading is kept for the direct participation $\theta_r = 0.2$, but a different safety loading is used for the contracts with the cedents with $\theta_1 = \theta_2 = \theta_3 = \theta_4 = \theta$. Figure 13 shows the variation of the optimal profit and Figure 14 gives the resulting δ_r^{h*} and Δ_c^* for $h = 1, 2, 3$ and $c = 1, 2, 3, 4$ as a function of the safety loading $\theta \in [0, 0.4]$. We can see that when increasing the safety loading for the contracts with the cedents from 0 to 0.4, the direct participations of the reinsurer in the second and third layer decrease from $\delta_r^{2*} = 0.072$ and $\delta_r^{3*} = 0.013$ to 0 and they get substituted by the participation on the cedents' contracts. It is worth noting that it is never optimal to have a participation in the contract with Cedent 2 for the entire range of the safety loading, even if this is the cedent with the second highest profit for the reinsurer, as the constraints also play a role in the substitution effect in this case.

We also explore the sensitivity of the solution with respect to the values used in the risk tolerance limits t_j. In this case, we define the risk tolerance limits for the same value of p_j as before but with $t_1 = 50b$, $t_2 = 75b$, and $t_3 = 250b$. Figure 15 shows the variation of the optimal profit and Figure 16 presents δ_r^{h*} and Δ_c^* for $h = 1, 2, 3$ and $c = 1, 2, 3, 4$ as a function of $b \in [0.1, 2.5]$. Clearly, the profit is an increasing function of b, given that the higher the tolerance limits are, the participations on the layers and the contracts can increase and lead to more profits. We also observe an increasing behavior on δ_r^{h*} with respect to b,
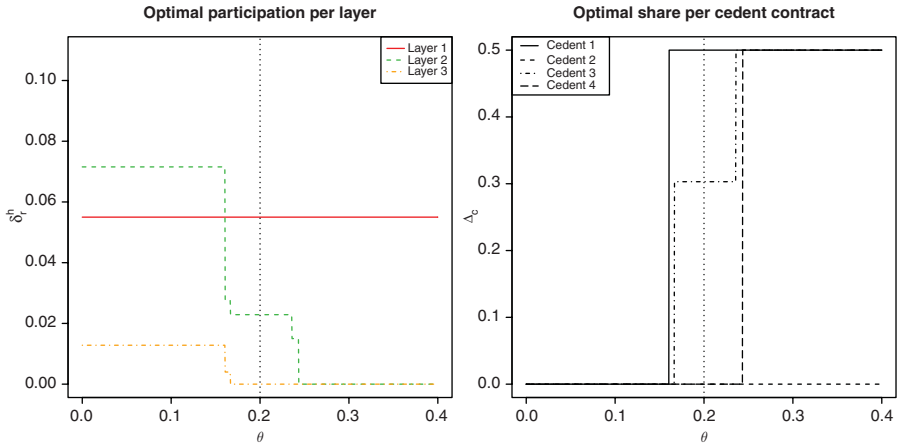
FIGURE 14: δ_r^{h*} (left) and Δ_c^* (right) as function of θ for $\theta_r = 0.2$.
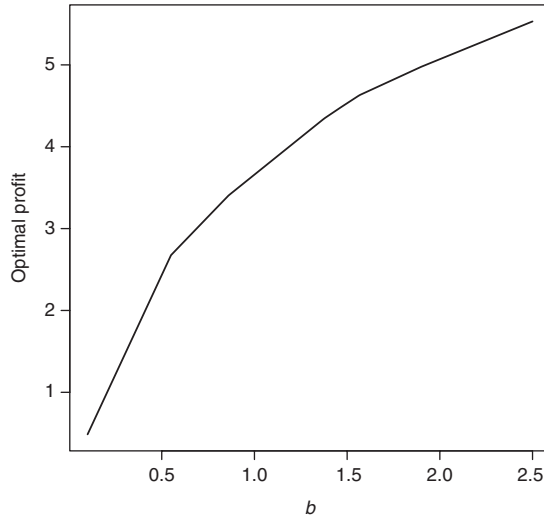

FIGURE 15: Optimal profit as function of b.

so that for a sufficiently high value of the tolerance limits it is optimal to participate up to the maximum possible value in all layers. In contrast, for Δ_c the maximum value Δ^{UP} is reached for all cedents for $b \geq 1.9$, but the relationship among Δ_c^* and b is not necessarily monotonic, as observed for Cedents 2 and 3.

Finally, we want to evaluate the sensitivity of the parameters λ and α from the frequency and severity distributions. Figure 17 shows the variation of the optimal profit and Figures 18 and 19 give δ_r^{h*} and Δ_c^* for $h = 1, 2, 3$ and $c = 1, 2, 3, 4$ as a function of $\alpha \in [0.7, 2.5]$ and $\lambda \in [0.5, 5]$. We can observe that the profit increases for small values of α and big values of λ. In this region, the number of effective constraints reduces to one given that F_X is a decreasing
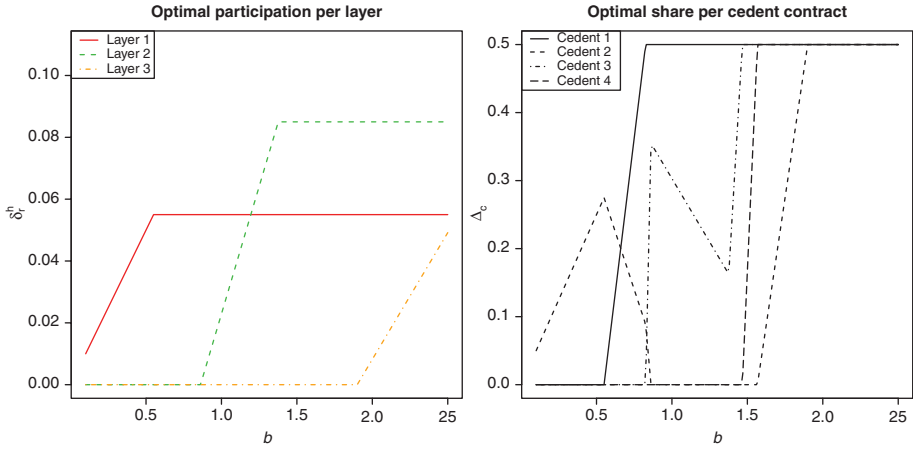
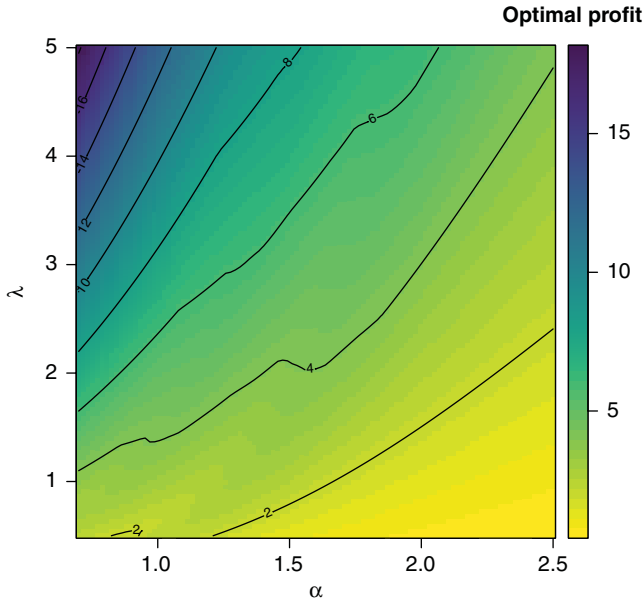FIGURE 16: δ_r^{h*} (left) and Δ_c^* (right) as function of b.

FIGURE 17: Expected profit for different values of the parameters $\alpha \in [0.7, 2.5]$ and $\lambda \in [0.5, 5]$.

function of α and P_N^{-1} increases with λ, so that equation (5.4) is only fulfilled by p_1. The direct participation of the reinsurer in the first layer is always the maximum possible $\delta^{1,UP} = 0.055$, while for the other two layers it decreases to zero in the region with fewer constraints. Nevertheless, the relationship is not monotone, and it is influenced by the constraints and the interactions with the cedents' contracts. The values Δ_c exhibit a similar behavior without a monotone pattern, for instance for Δ_3^* we can see that the maximum is attained in
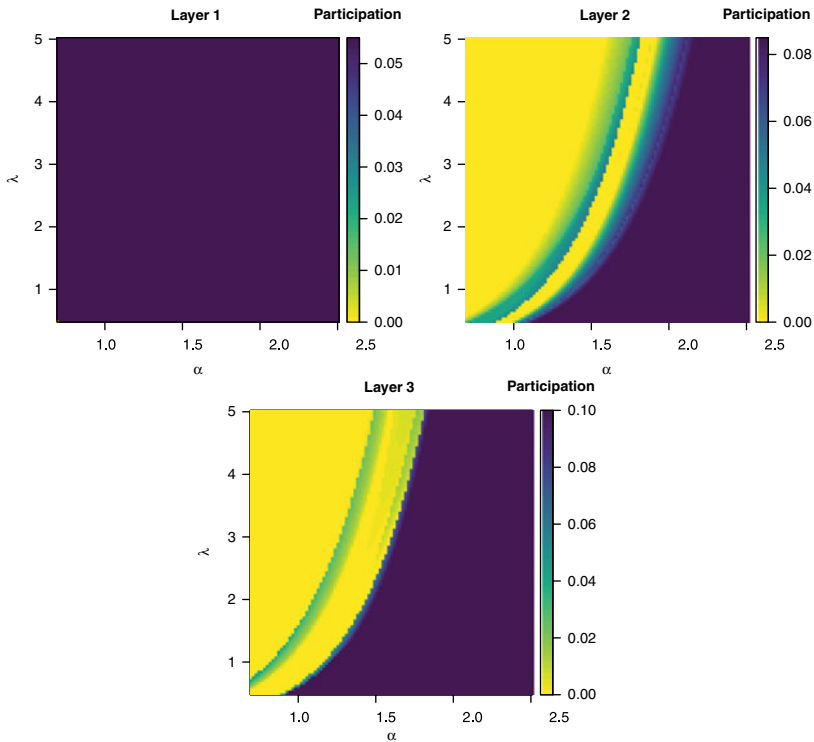
FIGURE 18: Optimal participations δ_r^{h*} for different values of the parameters $\alpha \in [0.7, 2.5]$ and $\lambda \in [0.5, 5]$.

the region with the three constraints, it decreases and is reached again before falling down to zero.

7. CONCLUSION

In this paper, we analyzed data from the marine liability insurance market. For the frequency modeling, we studied both homogeneous and inhomogeneous Poisson processes, indicating a decreasing intensity over time as expected from the general trend on the marine liability market. The analysis of the claim severity clearly supports the heavy-tailedness of the marine liability line of business. We considered various approaches for the estimation of the extreme value index, including bias corrections and censoring techniques due to many open claims, and the resulting estimate is typically around 1, implying a severity distribution with infinite variance and possibly even infinite mean.

We then introduced a profit optimization problem that large reinsurance companies in markets like marine liability or US flood insurance face. The profit optimization problem becomes a linear and a quadratic program when the reinsurer uses the expected value and the variance premium principle, respectively. We illustrated solutions for certain choices of the involved parameters and studied the sensitivity of the optimal solution with respect to the model parameters.
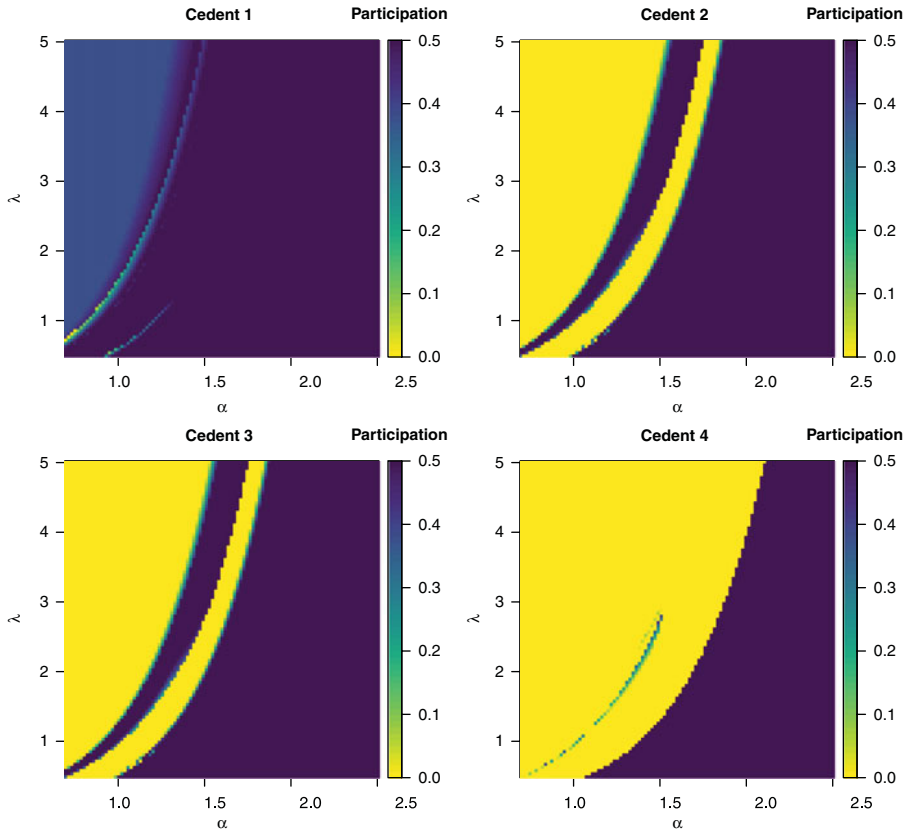
FIGURE 19: Optimal participations Δ_c^* for different values of the parameters $\alpha \in [0.7, 2.5]$ and $\lambda \in [0.5, 5]$.

In future research, one may consider other premium principles, although the form of the optimization problem will then typically be considerably more complicated. Risk tolerance limits based on aggregate exceedance probabilities (AEPs) instead of OEPs could also be considered, but such AEPs will lead to nonlinearities in the constraints as well. Nevertheless, if the probability of having two or more claims is very small, OEP and AEP values are often very similar in any case, see for example, Homer and Li (2017). In the present paper, the optimization problem was formulated in terms of maximizing expected profit given OEP risk constraints. It will be interesting in future research to also consider other tail risk measures, such as Value-at-Risk and Expected Shortfall and investigate the effects on the optimal solutions.

ACKNOWLEDGMENTS

Jan Beirlant, and Simon Lanthaler for helpful comments. The authors would also like to thank the reviewers and the editor for their valuable and constructive comments.

NOTES

1. The current structure of the IG GXL program can be looked up on http://www.igpandi.org/reinsurance.

2. See http://www.fema.gov/nfip-reinsurance-program.

3. Historically, this unusual renewal date was set because it was the date when the Baltic Sea was expected to be ice-free, an important event at the time when P&I clubs were largely concentrated in Northern Europe.

REFERENCES

AGCS (2019) Safety and Shipping Review 2019. An annual review of trends and developments in shipping losses and safety. Allianz Global Corporate & Specialty (AGCS).

ALBRECHER, H., BEIRLANT, J. and TEUGELS, J.L. (2017) *Reinsurance: Actuarial and Statistical Aspects*. Wiley Series in Probability and Statistics, Chichester, UK: John Wiley & Sons Ltd.

ALBRECHER, H., BLADT, M., KORTSCHAK, D., PRETTENTHALER, F. and SWIERCZYNSKI, T. (2019) Flood occurrence change-point analysis in the paleoflood record from Lake Mondsee (NE Alps). *Global and Planetary Change*, **178**, 65–76.

BEIRLANT, J. and GOEGEBEUR, Y. (2003) Regression with response distributions of Pareto-type. *Computational Statistics & Data Analysis*, **42**(4), 595–619.

COWLING, A. and HALL, P. (1996) On pseudodata methods for removing boundary effects in kernel density estimation. *Journal of the Royal Statistical Society. Series B (Methodological)*, **58**(3), 551–563.

DANTZIG, G.B. (1951) Maximization of a linear function of variables subject to linear inequalities, chapter. In *Activity Analysis of Production and Allocation*, pp. 339–347. New York: John Wiley & Sons Ltd.

DEKKERS, A.L.M., EINMAHL, J.H.J. and DE HANN, L. (1989) A moment estimator for the index of an extreme-value distribution. *Annals of Statistics*, **17**(4), 1833–1855.

DIGGLE, P. (1985) A kernel method for smoothing point process data. *Journal of the Royal Statistical Society: Series C (Applied Statistics)*, **34**(2), 138–147.

EINMAHL, J., FILS-VILLETARD, A. and GUILLOU, A. (2008) Statistics of extremes under random censoring. *Bernoulli*, **14**(1), 207–227.

EINMAHL, J.H.J., DE HAAN, L. and ZHOU, C. (2016) Statistics of heteroscedastic extremes. *Journal of the Royal Statistical Society. Series B (Statistical Methodology)*, **78**(1), 31–51.

FARR, D., SUBASINGHE, H., NEWMAN, A., GINGELL, C., STUART, D., MONTAGUE, E., PEACOCK, E., DAWSON, G., RAMA, G., GARDNER, J., PATEL, K., FRONTADO, L., LO, M., HARIA, S., ASHRAF, S., HODKINSON, S. and HARTINGTON, T. (2014) Marine and energy pricing. *GIRO Conference*.

FUTTERKNECHT, O., PAIN, D. and TURNER, G. (2013) Navigating recent developments in marine and airline insurance. Sigma. Swiss Re (4).

GIRO (2011) Risk appetite for a general insurance undertaking. Risk Appetite Working Party (GIRO).

HALL, P. (1982) On some simple estimates of an exponent of regular variation. *Journal of the Royal Statistical Society. Series B (Methodological)*, **44**(1), 37–42.

HILL, B.M. (1975) A simple general approach to inference about the tail of a distribution. *Annals of Statistics*, **3**(5), 1163–1173.

HOLLAND, D.M. (2009) A brief history of reinsurance. *Reinsurance News*, Special Edition, **65**, 4–29.

HOMER, D. and LI, M. (2017) *Notes on Using Property Catastrophe Model Results*. Casualty Actuarial Society E-Forum 2.

IGP&I (2015) Annual Review 2014/2015. International Group of P&I Clubs (IGP&I).

IGP&I (2017) Annual Review 2016/2017. International Group of P&I Clubs (IGP&I).

ITOPF (2019) Oil Tanker Spill Statistics 2018. The International Tanker Owners Pollution Federation Limited (ITOPF).

KAAS, R., GOOVAERTS, M., DHAENE, J. and DENUIT, M. (2008) *Modern Actuarial Risk Theory. Using R*, *Second Edition*. Berlin: Springer-Verlag.

LLOYDS (2013) *The Challenges and Implications of Removing Shipwrecks in the 21st Century*. London, UK: Lloyd's.

LUENBERGER, D.G. and YE, Y. (2008) *Linear and Nonlinear Programming*, *Third Edition*. International Series in Operations Research & Management Science. New York: Springer.

MCNEIL, A.J. (1997) Estimating the tails of loss severity distributions using extreme value theory. *Astin Bulletin*, **27**(1), 117–137.

MERZ, B., NGUYEN, V.D. and VOROGUSHYN, S. (2016) Temporal clustering of floods in germany: Do flood-rich and flood-poor periods exist? *Journal of Hydrology*, **541**(B), 824–838.

MITCHELL-WALLACE, K., JONES, M., HILLIER, J. and FOOTE, M. (2017) *Natural Catastrophe Risk Management and Modelling. A Practitioner's Guide*. Chichester: John Wiley & Sons Ltd.

SELTMANN, A. (2019) Global marine insurance report 2019. *International Union of Marine Insurance (IUMI) Conference*.

SHEATHER, S.J. and JONES, M.C. (1991) A reliable data-based bandwidth selection method for kernel density estimation. *Journal of the Royal Statistical Society. Series B (Statistical Methodology)*, **53**(3), 683–690.

SWISS RE (2003) Marine Insurance. Swiss Re.

VANDERBEI, R.J. (2014) *Linear Programming. Foundations and Extensions*. *Fourth Edition*. International Series in Operations Research & Management Science. New York: Springer,.

WHITE, I.C. and MOLLOY, F.C. (2003) Factors that determine the cost of oil spills. *International Oil Spill Conference Proceedings*, Vol. 1, pp. 1225–1229.

WILLIAM GUEVARA-ALARCÓN (Corresponding author)
SCOR Switzerland Ltd
General Guisan Quai 26
8002 Zürich, Switzerland
and
Department of Actuarial Science
Faculty of Business and Economics
University of Lausanne
1015 Lausanne, Switzerland
E-Mail: wguevara@scor.com, wmguevaraa@unal.edu.co

HANSJÖRG ALBRECHER
Department of Actuarial Science
Faculty of Business and Economics
University of Lausanne
1015 Lausanne, Switzerland
and
Swiss Finance Institute
Lausanne, Switzerland
E-Mail: hansjoerg.albrecher@unil.ch

PARVEZ CHOWDHURY
SCOR Switzerland Ltd
General Guisan Quai 26
8002 Zürich, Switzerland
E-Mail: pchowdhury@scor.com